ELSEVIER

Biophysical Chemistry 134 (2008) 47–55

Biophysical Chemistry

http://www.elsevier.com/locate/biophyschem

# Olanzapine interaction with dipalmitoyl phosphatidylcholine (DPPC) and 1-palmitoyl-2-oleoyl phosphatidylserine (POPS) bilayer: A $^{13}C$ and $^{31}P$ solid-state NMR study ☆

Chen Song, Willy Nerdal *

*Department of Chemistry, University of Bergen, Allegaten 41, N-5007 Bergen, Norway*

Received 19 October 2007; received in revised form 8 January 2008; accepted 9 January 2008
Available online 17 January 2008

**Abstract**

Phospholipid bilayer interaction of olanzapine (OLZ), a thienobenzodiazepine derivative and an antipsychotic agent, has been studied with $^{13}C$ and $^{31}P$ solid-state NMR. A dipalmitoyl phosphatidylcholine (60%)/1-palmitoyl-2-oleoyl phosphatidylserine (40%) bilayer (DPPC(60%)/POPS (40%)) with 50 wt.% $H_2O$, with and without 10 mol% OLZ have been investigated. The results reveal that both the serine and the choline head groups are affected by OLZ interaction with the bilayer. The OLZ interaction with the serine and the choline head groups appears to be caused by electrostatic attraction to the serine head group carboxyl and repulsion of the choline head group positively charged nitrogen. $^{31}P$ MAS NMR experiments show the appearance of two new $^{31}P$ resonances both for the PS and the PC phosphorous in the presence of OLZ. Static $^{31}P$ NMR spectra demonstrate a decrease in chemical shift anisotropy (CSA) of the OLZ containing bilayer when in the liquid-crystalline phase and an increase in CSA when in the gel state.


*Keywords:* Solid-state NMR; $^{13}C$ NMR; $^{31}P$ NMR; DPPC/POPS; Bilayer; Olanzapine interaction

## 1. Introduction

Olanzapine (OLZ, see Scheme 1), a relatively new thienobenzodiazepine derivative, is widely used as an antipsychotic agent and has become one of the most commonly used atypical antipsychotics [1] with antagonism of dopamine $D_1$, muscarinic $M_{1-5}$, $\alpha_1$-adrenoceptors and histamine $H_1$ receptors [2]. OLZ exhibits relatively high affinity for several neurotransmitter receptors, such as $D_{1-5}$ dopaminergic, 5-$HT_{2A-2C}$ and 5-$HT_{3,6,7}$ serotonergic, $\alpha_1$-adrenoceptors and histamine $H_1$ [1–7], as well as moderate affinity for the five muscarinic receptor subtypes, $M_{1-5}$ [8]. The functional blockade of these receptors may contribute to its broad efficacy in the treatment of schizophrenia and related psychoses [9–12]. However, in therapeutic concentrations OLZ inhibits the integral membrane protein phospholipase D (PLD), that acts specifically on phosphatidylcholine [13], and elevates the serum creatine kinase (CK) level [14], the latter effect may cause or induce cell membrane damage. Furthermore, OLZ is found to elevate apolipoprotein-D (apoD) levels [15]. Thus, OLZ can interfere with phospholipid metabolism, in that apoD binds to arachidonic acid (AA) and cholesterol [16–18]. Recently, Parikh et al. [19] found that OLZ prevented loss of antioxidant enzymes in rat brain. Evans et al. [20] indicated that reduced levels of antioxidant enzymes can be associated with increased plasma lipid peroxides and reduced level of essential polyunsaturated fatty acids (EPUFA) in membranes, omega-3 fatty acids in particular. Studies of rats subjected to atypical antipsychotic agents (olanzapine, clozapine, and risperidone) demonstrate that they have antioxidant

*Abbreviations:* DPPC, 1, 2-dipalmitoyl-*sn*-glycerol-3-phosphatidylcholine; POPS, 1-palmitoyl-2-oleoyl-*sn*-glycerol-3-phosphatidylserine; PC, phosphatidylcholine; PS, phosphatidylserine; OLZ, olanzapine; MAS, magic angle spinning; NMR, nuclear magnetic resonance; CSA, chemical shift anisotropy.

☆ This work was supported by a grant from the Norwegian Research Council (NFR).

* Corresponding author. Department of Chemistry, University of Bergen, Allegaten 41, N-5007 Bergen, Norway. Tel.: +47 55 583353; fax: +47 55 589400.
*E-mail address:* Willy.Nerdal@kj.uib.no (W. Nerdal).

0301-4622/$ - see front matter © 2008 Elsevier B.V. All rights reserved.
doi:10.1016/j.bpc.2008.01.002

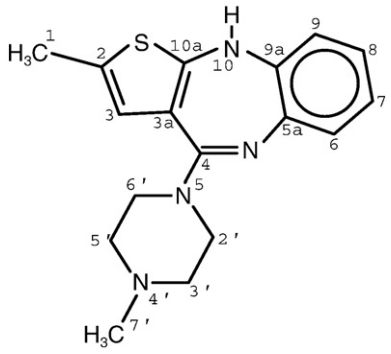

Scheme 1. Molecular structure of olanzapine (OLZ) with numbering of atoms.

effects, reduce lipid peroxidation [21,22] and affect membrane 5-$HT_2$ receptor affinity [23]. Furthermore, olanzapine, clozapine and risperidone were found to improve the levels of erythrocyte EPUFAs [24], possibly a contributing effect in the treatment of schizophrenia [25,26].

The activity of membrane proteins bound to lipid bilayers can be influenced by changes in phospholipid composition of the bilayer [27]. Therefore, it is likely that perturbation of the lipid bilayer by amphiphilic OLZ molecules can influence the activity of bilayer-bound proteins, even without direct interaction between the protein and the amphiphile. Consequently, some of the effects of OLZ on dopaminergic receptors [2] could be due to OLZ perturbation of the lipid bilayer that contains the receptor. The effects of OLZ on processes taking place in biological membranes are scarcely investigated. This is contrasted by the typical anti-psychotic agent chlorpromazine (CPZ), that has prompted several physiochemical studies of interactions with glycerophospholipids by various techniques, such as Electron Spin Resonance (ESR) [28], Electron Paramagnetic Resonance (EPR) [29], X-ray [30], and NMR [31–33].

In this study, $^{13}C$ [34] and $^{31}P$ [35] solid-state NMR techniques were employed to study the interaction of 10 mol% OLZ with a DPPC(60%)/POPS(40%) bilayer with 50 wt.% $H_2O$. Samples were pH adjusted to 7.4 in order to ensure that the serine head group carboxyl group is deprotonated (p*K*a of 4.4). In earlier studies we have carried out solid-state NMR experiments to investigate interaction of chlorpromazine with a bilayer with a PC and PS ratio of 1.5, i.e. 60 mol% PC and 40 mol% PS. Both $^{31}P$ and $^{13}C$ MAS NMR spectra demonstrated that this phospholipid PC/PS ratio simplifies identification of resonances acquired on such bilayers without and with amphiphile. A 10 mol% OLZ content in the DPPS/POPS bilayer of this study is well above what is found at the macroscopic level *in vivo* [36], but it is possible that lower OLZ concentrations may induce profound changes in bilayer architecture such as those outlined in this study. DPPC is a common lipid in the plasma membrane of eukaryotic cells and PS is the most abundant acidic lipids in mammalian cells. At a sample temperature of 43 °C both DPPC (Tc~41 °C) and POPS (Tc~16 °C) are in the liquid-crystalline phase. A PC(60%)/PS (40%) sample composition can be expected to be fully miscible in that phase diagrams for DMPS–DMPC [37] and DEPS–DEPC [38] mixtures were found highly miscible in both the gel and liquid-crystalline phases in the presence of only monovalant cations. However, in the presence of 30 mM calcium ions PS–PC samples containing 40–70% PS show both lamellar and cochleate structures at temperatures well above 37 °C and at lower temperatures (than 37 °C) two solid phases will form for samples with PS content up to about 40% PS [37].

## 2. Materials and methods

### 2.1. Chemicals

Olanzapine (OLZ, powder) was obtained from *SynFine* Research Inc. (Ontario, Canada), synthetic 1,2-dipalmitoyl-*sn*-glycero-3-phosphatidylcholine (DPPC, lyophilized powder) and synthetic 1-palmitoyl-2-oleoyl-*sn*-glycero-3-[phospho-L-serine] (POPS, lyophilized powder) were purchased from Avanti Polar Lipids Inc. (Birmingham, Alabaster, AL, USA). The lipids were used without further purification.

### 2.2. Sample preparation of DPPC(60%)/POPS(40%) and DPPC(54%)/POPS(36%)/OLZ(10%) bilayers with 50 wt.% $H_2O$

The desired amounts of DPPC and POPS to achieve a molar composition of 60% phosphatidylcholine and 40% phosphatidylserine bilayers were weighed into a plastic tube, dissolved in spectroscopic grade chloroform, dried under a stream of argon gas until a thin film around the bottom of the plastic tube was formed. This was followed by overnight lyophilization in a vacuum chamber to dryness. The sample of dry powder was then suspended in degassed distilled water, and counterions were added by using an equi-molar quantity to the serine headgroups of sodium perchlorate salt ($NaClO_4$). The perchlorate anion has been found to stabilize the liquid-expanded phase of DPPC monolayers without affecting the conformation and packing properties of the acyl chains [39]. (Addition of this amount of $NaClO_4$ proved to have no oxidizing effect on the bilayer samples). Subsequently, the lipid suspension of DPPC/POPS was divided into two equi-amount parts, and the appropriate amount of OLZ (dissolved in degassed distilled water) was added to obtain a bilayer sample of DPPC/POPS/OLZ with an OLZ content of 10 mol%. The suspensions contained multilamellar liposomes and unilamellar systems were obtained by ten freeze–thawing cycles from −196 to 22 °C. At the freeze–thawing stage, both samples were adjusted to a pH of 7.4 by adding a small amount of 0.05 M NaOH, and the bilayers were kept under an argon atmosphere and not exposed to air and light. Thus, a sample of PC(54%)/PS(36%)/OLZ(10%) was obtained as well as the corresponding sample without OLZ (PC(60%)/PS(40%)). Subsequently, the samples were subjected to 24 h of lyophilization giving partially hydrated liposomes with a hydration level of 12 water molecules per lipid molecule (determined by $^1H$ MAS NMR). The appropriate amount of degassed distilled water was added to the each sample to obtain hydrated bilayers with 50 wt.% $H_2O$ followed by equilibration above the samples gel-to-liquid-crystalline transition temperatures ($T_c$) at 50 °C for 48 h and packed into NMR rotors.

### 2.3. NMR Spectroscopy

#### 2.3.1. $^{13}C$ MAS NMR Spectroscopy

The $^{13}C$ MAS NMR experiments were obtained at 125.76 MHz on a Bruker 500 MHz Ultrashield Plus instrument (11.75 T) equipped with magic angle spinning (MAS) hardware and by the use of $ZrO_2$ rotors with a diameter of 4 mm. Experiments were done at a sample temperature of 43 °C, with a sample spinning rate of 2 kHz. (The sample temperature at this spinning rate was checked by measuring the gel-to-liquid-crystalline phase transition of a pure DPPC bilayer sample). The $^{13}C$ NMR experiments were carried out with high-power proton decoupling during the acquisition. In this study, experiments were carried out with a relaxation delay of 6 s between transients, and a total of 16,384 transients were accumulated for each experiment. The fids were multiplied with an exponential window function increasing the linewidth by 2 Hz to reduce noise prior to Fourier transformation.

$^{13}C$ spin-lattice relaxation time constants ($T_1$) were obtained by a modified inversion-recovery pulse sequence using a composite 180-pulse [40] to counteract potential problems associated with non-uniform excitation across the range of $^{13}C$ chemical shifts. A $^{13}C$ NMR 90-degree pulse was approximately 7–9 μs and the recycling time was set to five times the largest $T_1$, typically 10 s between transients, and 2048 transients accumulated at sample temperatures of 23, 33 and 43 °C, respectively. In order to obtain accurate relaxation data on the palmitic acyl chain methyl group, relaxation experiments employing a 50 s relaxation delay were also carried out with 32 transients.

#### 2.3.2. $^{31}P$ NMR Spectroscopy

$^{31}P$ experiments were carried out at 202.47 MHz on a Bruker 500 MHz Ultrashield Plus instrument. Magic angle spinning $^{31}P$ experiments were carried out with a rotor spinning rate of 2 kHz. Typically, 2048 transients with a relaxation delay of 5 s between transients were accumulated at the various temperatures ranging from 23–43 °C, and Fourier transformed without apodization in order to keep spectral resolution.

Static $^{31}P$ spectra were acquired on these bilayer samples at 27 and 43 °C with high-power decoupling during acquisition. Typically, 2048 transients were collected for each experiment with a relaxation delay of 6 s between transients. These fids

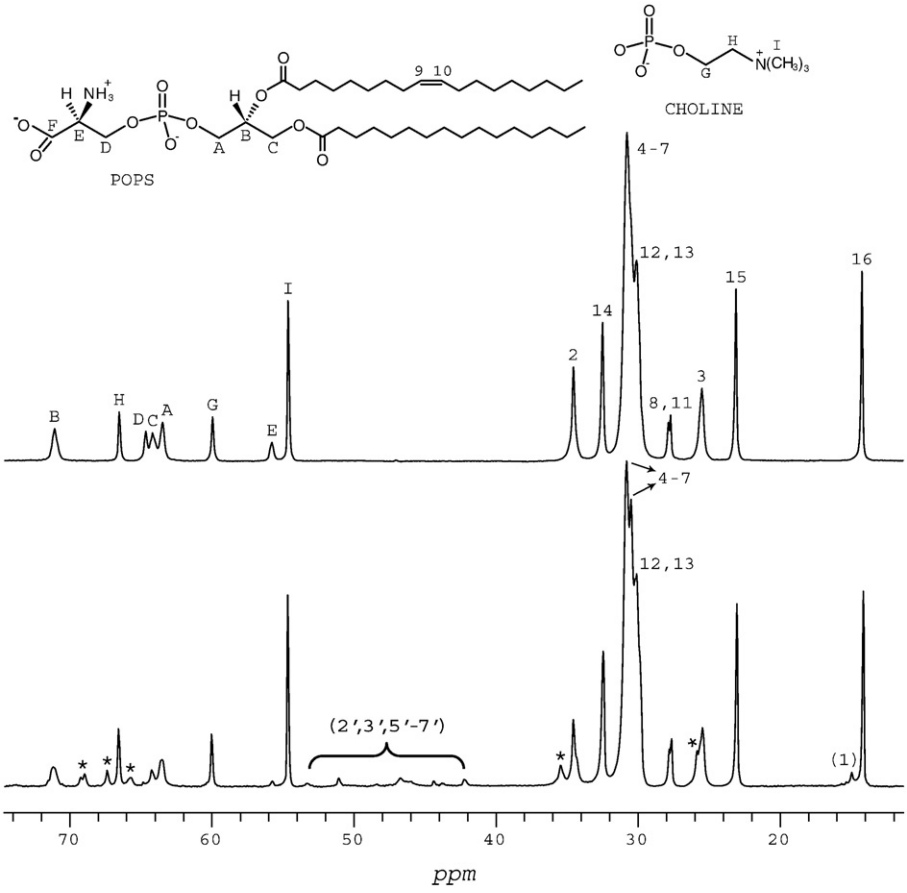


Fig. 1. $^{13}C$ MAS NMR spectra displaying the 0–74 ppm spectral region of bilayer samples at 43 °C. The molecular structure of POPS and of the PC head group/phosphorus (CHOLINE) are shown with capital letters next to glycerol and serine/choline head group carbons that correspond to resonance assignments in top spectrum. Top: Spectrum of DPPC(60%)/POPS (40%) sample at 50 wt.% $H_2O$. Glycerol and phospholipid head group resonances are labelled A-I, where the 12–38 ppm region is labelled with the palmitic (16:0) acyl chain resonances, as well as resonances 8 and 11 of the oleic acyl chain. The choline head group resonances G, H and I correspond to choline carbons α, β and the three nitrogen bound carbons, respectively. Bottom: Spectrum of DPPC(54%)/POPS(36%)/OLZ (10%) sample at 50 wt.% $H_2O$. Resonances labelled with an asterisk "*" denote new peaks when OLZ is present — compare with top spectrum. Some OLZ resonances are labelled with atom numbers in the parenthesis (2′, 3′, 5′–7′) and (1). See the text for details.

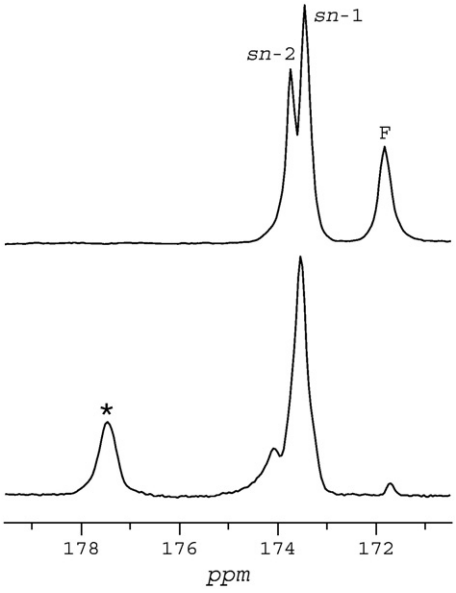


Fig. 2. Top: $^{13}$C MAS NMR spectrum of DPPC(60%)/POPS(40%) at 50 wt.% $H_2O$ and at a sample temperature of 43 °C. The two carbonyl resonances are labelled *sn*-1 and *sn*-2 and the serine carboxyl resonance is labelled F. Bottom: $^{13}$C MAS NMR spectrum of DPPC(54%)/POPS(36%)/OLZ(10%) at 50 wt.% $H_2O$ and at a sample temperature of 43 °C. The main part of the carboxyl resonance is shifted 5.8 ppm to higher ppm values (labelled with an asterisk "*") in the presence of OLZ.

were multiplied with an exponential window function increasing the linewidth by 50 Hz to reduce noise prior to Fourier transformation. The $^{31}$P chemical shift anisotropy was determined by assistance of computer simulations (Bruker Topspin 1.3). $^{31}$P relaxation data were obtained by employing the same pulse program as for $^{13}$C $T_1$ measurements at temperatures of 23–43 °C and with rotor spinning speed of 2 kHz. A $^{31}$P NMR 90-degree pulse was approximately 4–5 μs and the recycling time was set to five times the largest $T_1$, typically 8 s between a total of 1024 transients. The $^{31}$P chemical shifts were referenced to 85% phosphoric acid ($H_3PO_4$, 0 ppm).

## 3. Results

Comparison of the DPPC(54%)/POPS(36%)/OLZ(10%) bilayer sample spectrum in Fig. 1-bottom and a $^{13}$C MAS NMR spectrum of the pure OLZ powder with 15 wt.% $D_2O$ (data not shown), indicates that the resonances within the 42–52 ppm spectral region and the resonance at 16.79 ppm are OLZ carbon resonances [41]. Scheme 1 shows the chemical structure of OLZ, and corresponding assignments are used in Fig. 1-bottom spectrum (in brackets).

Fig. 1-top and -bottom display $^{13}$C MAS NMR spectra at 43 °C of DPPC(60%)/POPS(40%) and DPPC(54%)/POPS(36%)/OLZ (10%) bilayer samples, respectively. The 12–74 ppm spectral region is shown as well as the molecular structure of the POPS molecule together with capital letters next to glycerol and serine headgroup carbons corresponding to assignments of acyl chain $sp^3$ carbon resonances in spectrum of Fig. 1-top, some of these acyl chain resonances are also labelled in spectrum of Fig. 1-bottom. The palmitic acyl chain contributes 80% to the resonance intensities of the spectra and these are assigned in Fig. 1-top, as well as carbon resonances 8 and 11 of the oleic acyl chain. (The oleoyl chain carbon resonances 9 and 10, labelled in the POPS structure on top of Fig. 1, are presented in Fig. 3, see later). The molar composition of the bilayer gives a theoretical PC/PS peak ratio of 1.5, this is confirmed in the phospholipid head group (54–74 ppm) spectral region of Fig. 1-top where the choline resonance G and the serine resonance D show a 1.5 intensity ratio. The resonances labelled with an asterisk "*" in Fig. 1-bottom show phospholipid carbon resonances in the presence of OLZ. These resonances demonstrate OLZ interaction in the polar region of the DPPC/POPS bilayer. High molecular mobility is evident from the narrow lineshapes of the internal methylene $(CH_2)_n$ resonances. Fig. 2 displays the carbonyl/carboxyl spectral region of $^{13}$C MAS NMR spectra of bilayer samples DPPC(60%)/POPS (40%) and DPPC(54%)/POPS(36%)/OLZ(10%), top and bottom spectrum, respectively, at a sample temperature of 43 °C. In Fig. 2-top, the two carbonyl resonances can be identified (labelled *sn*-1 and *sn*-2) [42] as well as the serine carboxyl resonance, labelled F.

A comparison of the serine head group carboxyl F resonance, Fig. 2-top, with the OLZ containing bilayer spectrum of Fig. 2-bottom, makes it evident that the main part of this carboxyl resonance is shifted 5.80 ppm to higher ppm values (labelled

Table 1
$^{13}$C $T_1$ values (*s*) of the DPPC(60%)/POPS(40%) and DPPC(54%)/POPS(36%)/OLZ(10%) bilayers at 23, 33, and 43 °C

| Carbon (*s*) | DPPC/POPS | | | DPPC/POPS/OLZ | | |
|---|---|---|---|---|---|---|
| | °C | | | | | |
| | 23 | 33 | 43 | 23 | 33 | 43 |
| Carbonyl (1) | | | | | | |
| *sn*-1 C=O | 1.18 | 1.30 | 1.34 | 2.57 | 2.08 | 1.41 |
| *sn*-2 C=O | 1.55 | 1.60 | 1.77 | 0.88 | 0.36 | 0.42 |
| Carboxyl (F) | 1.03 | 1.55 | 1.66 | 1.41 | 1.88 | 2.51 |
| POPS C=C | | | | | | |
| $C_9$ | 0.55 | 0.59 | 0.71 | 0.69 | 0.73 | 0.81 |
| $C_{10}$ | 0.47 | 0.55 | 0.60 | 0.67 | 0.71 | 0.80 |
| Glycerol carbons | | | | | | |
| *sn*-1 (A) | 0.12 | 0.15 | 0.15 | 0.11 | 0.11 | 0.16 |
| *sn*-2 (B) | 0.36 | 0.39 | 0.50 | 0.57 | 0.72 | 0.87 |
| *sn*-3 (C) | 0.09 | 0.11 | 0.10 | 0.22 | 0.18 | 0.04 |
| Serine carbons | | | | | | |
| α *(D)* | 0.12 | 0.18 | 0.21 | 0.42 | 0.55 | 0.66 |
| β *(E)* | 0.39 | 0.37 | 0.40 | 0.49 | 0.68 | 0.93 |
| Choline carbons | | | | | | |
| α (G) | 0.18 | 0.21 | 0.23 | 0.29 | 0.28 | 0.33 |
| β (H) | 0.23 | 0.24 | 0.32 | 0.35 | 0.35 | 0.38 |
| $CH_3$ (I) | 0.25 | 0.30 | 0.36 | 0.32 | 0.36 | 0.49 |
| Palmitic carbons | | | | | | |
| 2 | 0.34 | 0.23 | 0.21 | 0.91 | 0.61 | 0.48 |
| 3 | 0.77 | 0.61 | 0.52 | 0.63 | 0.53 | 0.64 |
| 4–7 | 0.85 | 0.83 | 0.72 | 0.88 | 0.85 | 0.83 |
| 12, 13 | 0.68 | 0.71 | 0.70 | 0.64 | 0.65 | 0.74 |
| 14 | 1.05 | 1.11 | 1.17 | 0.99 | 1.04 | 1.24 |
| 15 | 0.92 | 0.99 | 1.08 | 0.96 | 1.24 | 1.19 |
| 16 | 1.73 | 1.88 | 3.51 | 2.20 | 2.25 | 4.35 |
| Oleic carbons | | | | | | |
| 8, 11 | 0.73 | 0.71 | 0.66 | 0.71 | 0.66 | 0.67 |

A-I: Resonances assigned in Figs. 1 and 2. The uncertainty in the $T_1$ values is estimated to ±10%.

with an asterisk "*" in Fig. 2-bottom). The corresponding change in $^{13}C$ $T_1$ values for the carbonyl resonance by adding OLZ to the bilayer suggests reduced phospholipid mobility (see Table 1). Furthermore, the changes in the *sn*-2 carbonyl chemical shift (see Fig. 2) and $T_1$ value (Table 1) strongly suggest phospholipid conformational changes as well as changes in the chemical environment for the phospholipids due to OLZ interaction [43]. This is supported by the observed behaviour of the serine carboxyl carbon, where the $T_1$ value (Table 1) of the carboxyl group at 171.7 ppm (Fig. 2-top) increases by 51% (from 1.66 s to 2.51 s) with the addition of OLZ, (Fig. 2-top) and the $T_1$ value of the new carboxyl resonance (labelled with an asterisk "*") at 177.5 ppm is found to be 3.24 s (Table 1).

Fig. 3 shows the 128–132 ppm spectral region of $^{13}C$ MAS NMR spectra of bilayer samples DPPC(60%)/POPS(40%) in Fig. 3-top and DPPC(54%)/POPS(36%)/OLZ(10%) in Fig. 3-bottom, at a sample temperature of 43 °C. In this spectral region, the C=C resonances of the oleic acyl chain carbons 9 and 10 in POPS are found, these are assigned in Fig. 3-top. The spectrum shown in Fig. 3-bottom of the DPPC(54%)/POPS (36%)/OLZ(10%) sample, displays a reduction of 0.2 ppm in the chemical shift separation ($\Delta\delta$) of carbons 9 and 10 resonances in the presence of OLZ (compare spectra in Fig. 3-top and -bottom). Furthermore, $T_1$ values for these oleic chain carbons 9 and 10 (Table 1) show that 10 mol% OLZ in the DPPC/POPS bilayer increases the $T_1$ values for these two C=C resonances in that carbon 9 experience an increase in $T_1$ from 0.71 s to 0.81 s (14%) and carbon 10 an increase in $T_1$ from 0.60 s to 0.80 s (33%), see Table 1. The small broad peak at 128.8 ppm in Fig. 3-bottom (labelled (2)) is an OLZ carbon resonance (see Scheme 1).

Fig. 4 displays the central band region of $^{31}P$ MAS NMR spectra acquired on bilayer sample DPPC(60%)/POPS(40%) in Fig. 4, left column, and on DPPC(54%)/POPS(36%)/OLZ (10%) in Fig. 4, right column. Sample temperatures are 23–43 °C, top row to bottom row. In Fig. 4, the experimental temperature is labelled to the left of the two spectra on the same row that are acquired at the given temperature. All spectra were obtained with a 2 kHz MAS spinning rate. The phosphatidylcholine and phosphatidylserine components are assigned in the spectra shown in the bottom row of Fig. 4, i.e. at 43 °C where the bilayer is in the liquid-crystalline state. In spectrum of DPPC/POPS sample displayed in Fig. 4, left column and bottom row, acquired at 43 °C, the chemical shift difference between PS and PC is 1.2 ppm. Existence of several lipid packing conformations is demonstrated in the somewhat broad appearance of the PS and PC resonances, even at 43 °C where the bilayer is in the liquid-crystalline phase. This tendency of several lipid packing conformations is becoming more pronounced at lower temperatures where the bilayer is in the gel phase, see Fig. 4, left column and top row, at a sample temperature of 23 °C where a new resonance appears in between the PS and PC resonances that are labelled in the liquid-crystalline bilayer phase (Fig. 4, left column and bottom row). The co-existence of several molecular packing arrangements in the DPPC/POPS bilayer at 23 °C is further supported

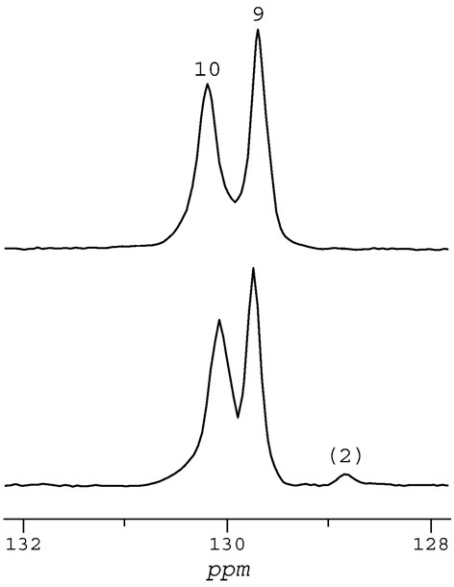


Fig. 3. Top: The 128–132 ppm spectral region of $^{13}C$ MAS NMR spectrum of bilayer sample DPPC(60%)/POPS(40%) at 50 wt.% $H_2O$ at a sample temperature of 43 °C. The C=C resonances of the oleic acyl chain carbons 9 and 10 of samples DPPC/POPS and DPPC/POPS/OLZ are assigned. Bottom: The 128–132 ppm spectral region of $^{13}C$ MAS NMR spectrum of bilayer sample DPPC(54%)/POPS(36%)/OLZ(10%) at 50 wt.% $H_2O$ at a sample temperature of 43 °C. The small broad peak at 128.78 ppm labelled (2) is an OLZ carbon resonance (see Scheme 1). See the text for details.

by the molecular composition of the bilayer that gives a theoretical PC/PS ratio of 1.5. Thus, the resonance between PS and PC of Fig. 4, left column and top row, at a sample temperature of 23 °C must have PS as well as PC phosphorous resonances contributing to the peak intensity.

Comparing spectrum of DPPC/POPS/OLZ sample shown in Fig. 4, right column and bottom row, i.e. at 43 °C, with corresponding spectrum of sample without OLZ shown in Fig. 4, left column and bottom row, resonances labelled a–c and d–f (Fig. 4, right column and bottom row) are PS and PC $^{31}P$ resonances, respectively. Of the three $^{31}P$ resonances attributed to PS, resonances a–c, the resonance labelled b is at the same chemical shift as the PS resonance in the spectrum without OLZ, see Fig. 4, left column and bottom row. Similarly, the resonance labelled d (Fig. 4, right column and bottom row) is at the same chemical shift as the resonance labelled PC in spectrum without OLZ, see Fig. 4, left column and bottom row. Thus, the presence of OLZ in the bilayer gives rise to chemical environments in the bilayer polar region that affect both PS and PC head groups. Furthermore, lowering sample temperature from 43 to 23 °C (Fig. 4, right column and top row) broadens all PS resonances (labelled a–c) and two PC resonances (labelled e and f) without affecting the PC resonance labelled d in Fig. 5, right column and bottom row. The OLZ affected $^{31}P$ resonances a–c of PS as well as e and f of PC are presumably broadened in spectra at lower temperatures due to low frequency motions caused by presence of OLZ. The conformational exchange rates can be estimated by the difference in resonance position (Hz) from resonances b of PS and d of PC to be in the 5–9 ms range.

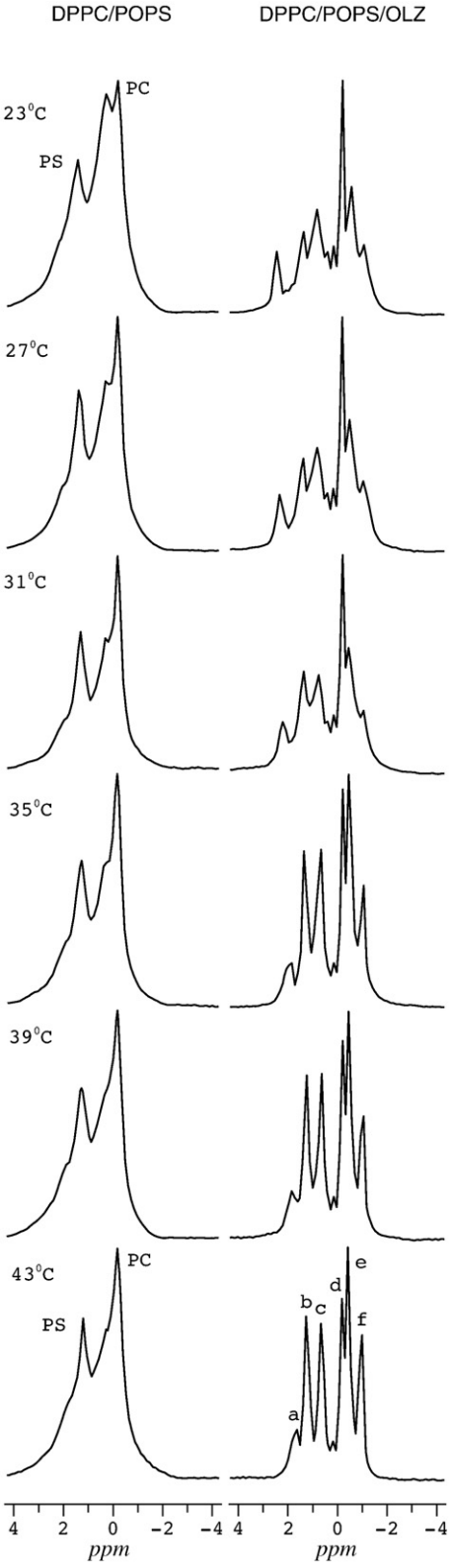


Fig. 4. $^{31}$P MAS NMR spectra of samples DPPC(60%)/POPS(40%) with 50 wt.% $H_2O$ (left column), and DPPC(54%)/POPS(36%)/OLZ(10%) with 50 wt.% $H_2O$ (right column) between sample temperatures 23 and 43 °C. The experimental temperature is labelled on the left of the row of corresponding spectra. All spectra were obtained with a 2 kHz MAS spinning rate. The phosphatidylserine (PS) and phosphatidylcholine (PC) resonances in the OLZ containing sample are assigned a–c and d–f, respectively, in the spectrum acquired at a sample temperature of 43 °C (right column–bottom row spectrum). See the text for details.

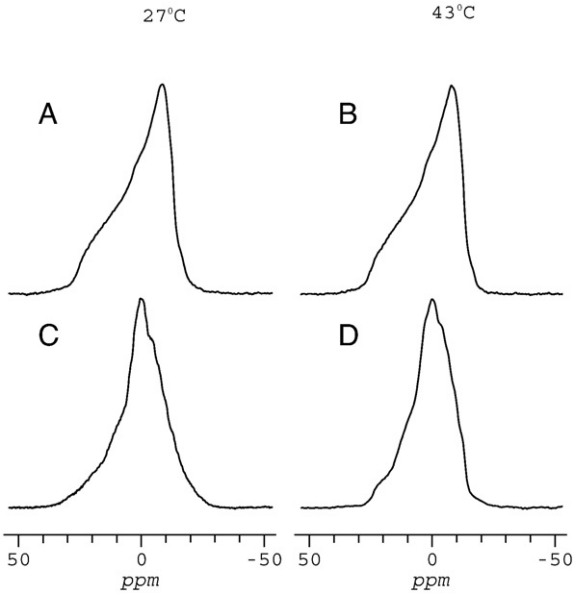


Fig. 5. Static $^{31}$P spectra of DPPC(60%)/POPS(40%) with 50 wt.% $H_2O$ at A: 27 °C and B: 43 °C. Static $^{31}$P spectra of DPPC(54%)/POPS (36%)/OLZ (10%) with 50 wt.% $H_2O$ at C: 27 °C and D: 43 °C. See the text for details.

$^{31}$P $T_1$ values of the central band peaks displayed in Fig. 4, listed in Table 2, show that both PS and PC phosphorous mobilities are sensitive to sample temperature. The $^{31}$P $T_1$ values for all of the phosphatidylserine resonances decrease with increasing temperature, indicating an increase in phosphorous mobility (slow motional regime). This behaviour is contrasted by the OLZ containing sample, where some $T_1$ values increase and other decrease with increasing temperature. The $T_1$ value of the peak labelled PC in Fig. 4, left column, decreases from 1.04 s at 23 °C to 0.59 s at 35 °C and then increases to 0.74 s at 39 °C and 0.78 s at 43 °C.

Fig. 5 shows static $^{31}$P spectra of samples acquired at 27 °C in Fig. 5-A and -C and at 43 °C in Fig. 5-B and -D, respectively. The spectra of DPPC(60%)/POPS(40%) are shown in Fig. 5-A and -B and the spectra of DPPC(54%)/POPS(36%)/OLZ(10%) are shown in Fig. 5-C and -D.

Table 2
$^{31}$P $T_1$ values ($s$) of the DPPC(60%)/POPS(40%) and the DPPC(54%)/POPS (36%)/OLZ(10%) bilayer

| | DPPC/POPS | | DPPC/POPS/OLZ[a] | | | | | |
|---|---|---|---|---|---|---|---|---|
| | | | PS | | | PC | | |
| | PS | PC | a | b | c | d | e | f |
| | | | (1.73) | (1.25) | (−0.66) | (−0.20) | (−0.42) | (−0.97) |
| 23 | 0.96 | 1.04 | 0.88 | 1.00 | 0.99 | 0.72 | 0.68 | 0.94 |
| 27 | 0.88 | 0.94 | 0.80 | 0.76 | 0.93 | 0.79 | 0.68 | 0.95 |
| 31 | 0.76 | 0.65 | 0.82 | 0.77 | 0.88 | 0.78 | 0.76 | 0.83 |
| 35 | 0.64 | 0.59 | 0.76 | 0.73 | 0.83 | 1.09 | 0.75 | 0.81 |
| 39 | 0.64 | 0.74 | 0.72 | 0.66 | 0.81 | 1.24 | 0.79 | 0.63 |
| 43 | 0.61 | 0.78 | 0.67 | 0.54 | 0.71 | 1.96 | 0.88 | 0.62 |

Sample temperatures are 23–43 °C.
See Fig. 5-right column and bottom row. The uncertainty in the $T_1$ values is estimated to ±10%.
[a] Resonances a–f with chemical shifts (ppm) in parentheses.

The $^{31}$P CSA values of DPPC(60%)/POPS(40%) (Fig. 5-A and -B) at 27 and 43 °C are 45.0 and 41.4 ppm, respectively. Incorporation of OLZ in the bilayer causes a diverse change of the bilayer's CSA demonstrated by the $^{31}$P CSA spectra of DPPC(54%)/POPS(36%)/OLZ(10%) shown in Fig. 5-C and -D, an increase in CSA to 51.0 ppm at 27 °C and a reduction to 37.9 ppm at 43 °C. Furthermore, the changed shape of the static $^{31}$P spectrum upon interaction with OLZ at 27 °C, compare spectra in Fig. 5-A and -C, where the latter is broader at both the low- and the high-field edges of the resonance, and more narrow in between, compared to the pure DPPC(60%)/POPS(40%) bilayer spectrum (Fig. 5-A), indicates different OLZ interaction with the PC and PS phospholipids in the gel state. At 43 °C, see Fig. 5-B and -D, OLZ interaction causes an overall decrease in CSA with less change in overall appearance in peak shape.

## 4. Discussion

A positively charged amphiphile located in the polar region of the bilayer [44] will push the choline head group of PC towards the surrounding water i.e. away from the plane of the bilayer, and thus, increase the corresponding $^{31}$P CSA value. Effects of some tricyclic antidepressants on head group order, conformation and dynamics of phospholipids have been found by the use of solid-state NMR [45]. The corresponding effect of a positively charged amphiphile on the orientation of a PS head group would be an observed reduction of the PS $^{31}$P CSA due to the serine negatively charged carboxyl being pulled towards the plane of the bilayer. In the liquid-crystalline phase, at 43 °C, OLZ reduces the CSA by 3.5 ppm in comparison to the observed CSA at 27 °C, where DPPC is in the gel state. Thus, indicating OLZ interaction with the PS head group.

The results of this study reveal that the serine head group is directly affected by OLZ interaction with the DPPC/POPS bilayer, and that the OLZ interaction with PS is to a great extent caused by electrostatic attraction to the serine head group. The serine head group carbon resonances (resonances D and E in Fig. 1-bottom) are greatly reduced in the presence of OLZ, whereas the choline head group resonances (resonances G, H and I in Fig. 1-bottom) display no such intensity reduction when the bilayer interacts with OLZ.

The 5.8 ppm chemical shift change to lower magnetic field (increased ppm value) displayed by the POPS serine head group carboxyl carbon resonance in the presence of 10 mol% OLZ can be explained by effects of electrostatic attraction between the negative carboxylate anion of PS and the positively charged OLZ. The positively charged site will be the 4′ nitrogen atom (see Scheme 1) of the piperazine ring and this will increase the chemical shift of the carboxyl carbon [46]. Furthermore, it cannot be ruled out that a change in the overall serine head group orientation when OLZ is present in the polar region of the bilayer changes the chemical shift of the carboxyl carbon to higher ppm values. An alternative explanation is that the OLZ aromatic ring is located next to the carboxyl carbon i.e. the ring current of the OLZ causes increased magnetic field at the serine carboxyl and thus the observed change to a 5.8 ppm higher chemical shift. Such effects are reported on membrane interaction of transmembrane peptides with tryptophan residues causing phospholipid protons located up to ~5 Å above/below the tryptophan ring to shift to lower ppm values [47].

The experiments of this study were carried out at a sample pH of 7.4 were a neutral and a positively charged form of OLZ are present at equal amounts [48] in that OLZ has p*K*a values of 7.4 and 4.7. The $^{31}$P MAS NMR experiments presented in Fig. 4 show two (major) new $^{31}$P resonances both for the PS and the PC phosphorous in the presence of OLZ. The slight increase in POPS $T_1$ values in the presence of OLZ might indicate that the POPS–OLZ interaction reduces the axial rotational motion of the POPS lipids, this could make the $T_1$ relaxation mechanism less efficient [49].

Furthermore, OLZ displays polymorphism and can form both dehydrated and hydrated dimers in the solid-state [40,50]. However, the relatively low OLZ content of 10 mol% in the DPPC/POPS bilayer of this study makes OLZ dimerization less likely. The static $^{31}$P NMR spectra presented in Fig. 5 demonstrate a substantial decrease in CSA of the OLZ containing bilayer. Thus, it can be concluded that incorporation of OLZ changes the lipid head group conformation/dynamics resulting in the observed decrease in the CSA span. The corresponding increased phospholipid head group mobilities producing such a CSA reduction by the presence of OLZ could very well lead to a changed lateral phospholipid organization of the bilayer [51]. In fact, the $^{31}$P MAS NMR spectra presented in Fig. 4 indicate that imperfections in DPPC and POPS mixing (see Fig. 4, left column and top row) are reduced in the presence of OLZ (see Fig. 4, right column and top row). Furthermore, OLZ interaction with phospholipid monolayers has recently been investigated and found to be substantial, in agreement with the findings of this NMR study on bilayers [52].

## References

[1] N.A. Moore, N.C. Tye, M.S. Axton, F.C. Risius, The behavioral pharmacology of olanzapine, a novel "atypical" antipsychotic agent, J. Pharmacol. Exp. Ther. 262 (1992) 545–551.
[2] F.P. Bymaster, D.L. Nelson, N.W. DeLapp, J.F. Falcone, K. Eckols, L.L. Truex, M.M. Foreman, V.L. Lucaites, D.O. Calligaro, Antagonism by olanzapine of dopamine $D_1$, serotonin$_2$, muscarinic, histamine $H_1$ and $\alpha_1$-adrenergic receptors in vitro, Schizophr. Res. 37 (1999) 107–122.
[3] A. Fuller, H.D. Snoddy, Neuroendocrine evidence for antagonism of serotonin and dopamine receptors by olanzapine (LY170053), an antipsychotic drug candidate, Res. Commun. Chem. Pathol. Pharmacol. 77 (1992) 87–93.
[4] F.P. Bymaster, D.O. Calligaro, J.F. Falcone, R.D. Marsh, N.A. Moore, N.C. Tye, P. Seeman, D.T. Wong, Radioreceptor binding profile of the atypical antipsychotic olanzapine, Neuropsychopharmacology 14 (1996) 87–96.
[5] F.P. Bymaster, K.W. Perry, D.L. Nelson, D.T. Wong, K. Rasmussen, N.A. Moore, D.O. Calligaro, Olanzapine: a basic science update, Br. J. Psychiatry Suppl. 37 (1999) 36–40.
[6] B.L. Roth, S.C. Craigo, M.S. Choudhary, A. Uluer, F.J. Monsma Jr., Y. Shen, H.Y. Meltzer, D.R. Sibley, Binding of typical and atypical antipsychotic agents to 5-hydroxytryptamine-6 and 5-hydroxytryptamine-7 receptors, J. Pharmacol. Exp. Ther. 268 (1994) 1403–1410.
[7] F.P. Bymaster, J.F. Falcone, D. Bauzon, J.S. Kennedy, K. Schenck, N.W. DeLapp, M.L. Cohen, Potent antagonism of 5-$HT_3$ and 5-$HT_6$ receptors by olanzapine, Eur. J. Pharmacol. 430 (2001) 341–349.

[8] F.P. Bymaster, J.F. Falcone, Decreased binding affinity of olanzapine and clozapine for human muscarinic receptors in intact clonal cells in physiological medium, Eur. J. Pharmacol. 390 (2000) 245–248.
[9] B. Fulton, K.L. Goa, Olanzapine. A review of its pharmacological properties and therapeutic efficacy in the management of schizophrenia and related psychoses, Drugs 53 (1997) 281–298.
[10] G.D. Tollefson, C.M. Beasley Jr., P.V. Tran, J.S. Street, J.A. Krueger, R.N. Tamura, K.A. Graffeo, M.E. Thieme, Olanzapine versus haloperidol in the treatment of schizophrenia and schizoaffective and schizophreniform disorders: results of an international collaborative trial, Am. J. Psychiatry 154 (1997) 457–465.
[11] M. Tohen, T.M. Sanger, S.L. McElroy, G.D. Tollefson, K.N.R. Chengappa, D.G. Daniel, F. Petty, F. Centorrino, R. Wang, S.L. Grundy, M.G. Greaney, T.G. Jacobs, S.R. David, V. Toma, Olanzapine HGEH study group, Olanzapine versus placebo in the treatment of acute mania, Am. J. Psychiatry 156 (1999) 702–709.
[12] C.M. Beasley Jr., G. Tollefson, P. Tran, W. Satterlee, T. Sanger, S. Hamilton, Olanzapine HGAD study group, Olanzapine versus placebo and haloperidol: acute phase results of the North American double-blind olanzapine trial, Neuropsychopharmacol. 14 (1996) 111–123.
[13] M. Krzystanek, H.I. Trzeciak, I. Krupka-Matuszczyk, E. Krzystanek, Antidepressant-like influence of olanzapine on membrane phospholipase D activity in rat brain, Eur. Neuropsychopharmacol. 12 (2002) 297–298.
[14] K. Melkersson, Serum creatine kinase levels in chronic psychosis patients — a comparison between atypical and conventional antipsychotics, Prog. Neuro-Psychopharmacol. and Biol. Psychiat. 30 (2006) 1277–1282.
[15] M.M. Khan, V.V. Parikh, S.P. Mahadik, Antipsychotic drugs differentially modulate apolipoprotein D in rat brain, J. Neurochem. 86 (2003) 1089–1100.
[16] J.K. Boyles, L.M. Notterpek, M.R. Wardell, S.C. Rall Jr., Identification, characterization and tissue distribution of apolipoprotein D in the rat, J. Lipid Res. 31 (1990) 2243–2256.
[17] P.P. Desai, C.H. Bunker, F.A.M. Ukoli, M.I. Kamboh, Genetic variation in the apolipoprotein D gene among African blacks and its significance in lipid metabolism, Atherosclerosis 163 (2002) 329–338.
[18] W.Y. Ong, C.P. Lau, S.K. Leong, U. Kumar, S. Suresh, S.C. Patel, Apolipoprotein D gene expression in the rat brain and light and electron microscopic immunocytochemistry of apolipoprotein D expression in the cerebellum of neonatal, immature and adult rats, Neuroscience 90 (1999) 913–922.
[19] V.V. Parikh, M.M. Khan, S.P. Mahadik, Differential effects of antipsychotics on expression of antioxidant enzymes and membrane lipid peroxidation in rat brain, J. Psychiatric Res. 37 (2003) 43–51.
[20] D.R. Evans, V.V. Parikh, M.M. Khan, C. Coussons, P.F. Buckley, S.P. Mahadik, Red blood cell membrane essential fatty acid metabolism in early psychotic patients following antipsychotic drug treatment, Prostaglandins Leukot. Essent. Fat. Acids 69 (2003) 393–399.
[21] S.P. Mahadik, D.R. Evans, H. Lal, Oxidative stress and role of antioxidant and ω-3 essential fatty acid supplementation in schizophrenia, Prog. Neuro-Psychopharmacol. and Biol. Psychiat. 25 (2001) 463–493.
[22] S.P. Mahadik, D.R. Evans, A. Terry, W.D. Hill, Neuroprotective actions of atypical antipsychotics in schizophrenia: improved cognitive performance and underlying mechanisms of action, Schizophr. Res. 49 (Suppl. 1) (2001) 94.
[23] A.C. Rego, C.R. Oliveira, Influence of lipid peroxidation on [$^3$H] ketanserin binding to 5-HT$_2$ prefrontal cortex receptors, Neurochem. Int. 27 (1995) 489–496.
[24] D.R. Evans, S.P. Mahadik, J. Akin, W. Evans, D. Jain, Cell membrane essential fatty acid status in drug-naive first-episode psychotic patients and its relation to outcome, Schizophr. Res. 49 (Suppl. 1) (2001) 83.
[25] M.M. Khan, D.R. Evans, V. Gunna, R.E. Scheffer, V.V. Parikh, S.P. Mahadik, Reduced erythrocyte membrane essential fatty acids and increased lipid peroxides in schizophrenia at the never-medicated first-episode of psychosis and after years of treatment with antipsychotics, Schizophr. Res. 58 (2002) 1–10.
[26] D.F. Horrobin, The membrane phospholipid hypothesis as a biochemical basis for the neurodevelopmental concept of schizophrenia, Schizophr. Res. 30 (1998) 193–208.
[27] A.G. Lee, Lipid–protein interactions in biological membranes: a structural perspective, Biochim. Biophys. Acta 1612 (2003) 1–40.
[28] M. Luxnat, H.-J. Galla, Partition of chlorpromazine into lipid bilayer membranes: the effect of membrane structure and composition, Biochim. Biophys. Acta 856 (1986) 274–282.
[29] K. Ondrias, A. Staško, V. Mišik, J. Reguli, E. Švajdlenka, Comparison of perturbation effect of propranolol, verapamil, chlorpromazine and carbisocaine on lecithin liposomes and brain total lipid liposomes. An EPR spectroscopy study, Chem.-Biol. Interact. 79 (1991) 197–206.
[30] M. Suwalsky, L. Gimenez, V. Saenger, F. Neira, X-ray studies on phospholipid bilayers. VIII. Interactions with chlorpromazine. HCl, Z. Naturforsch., c 43 (1988) 742–748.
[31] A.U. Gjerde, H. Holmsen, W. Nerdal, Chlorpromazine interaction with phosphatidylserines: a $^{13}$C and $^{31}$P solid-state NMR study, Biochim. Biophys. Acta 1682 (2004) 28–37.
[32] W. Nerdal, S.A. Gundersen, V. Thorsen, H. Høiland, H. Holmsen, Chlorpromazine interaction with glycerophospholipid liposomes studied by magic angle spinning solid state $^{13}$C-NMR and differential scanning calorimetry, Biochim. Biophys. Acta 1464 (2000) 165–175.
[33] C. Song, H. Holmsen, W. Nerdal, Existence of lipid microdomains in bilayer of dipalmitoylphosphatidylcholine (DPPC) and 1-stearoyl-2-docosahexenoylphosphatidylserine (SDPS) and their perturbation by chlorpromazine: a $^{13}$C and $^{31}$P solid-state NMR study, Biophys. Chemist. 120 (2006) 178–187.
[34] W.-g. Wu, L.-M. Chi, Comparisons of lipid dynamics and packing in fully interdigitated monoarachidoylphosphatidylcholine and non-interdigitated dipalmitoylphosphatidylcholine bilayers: cross polarization/magic angle spinning $^{13}$C-NMR studies, Biochim. Biophys. Acta 1026 (1990) 225–235.
[35] J.L. Browning, J. Seelig, Bilayers of phosphatidylserine: a deuterium and phosphorus nuclear magnetic resonance study, Biochemistry 19 (1980) 1262–1270.
[36] Z. Xia, G. Ying, A.L. Hansson, H. Karlsson, Y. Xie, A. Bergstrand, J.W. DePierre, L. Nässberger, Antidepressant-induced lipidosis with special reference to tricyclic compounds, Progr. Neurobiol. 60 (2000) 501–512.
[37] J.R. Silvius, J. Gagné, Calcium-induced fusion and lateral phase separations in phosphatidylcholine–phosphatidylserine vesicles. Correlation by calorimetric and fusion measurements, Biochemistry 23 (1984) 3241–3247.
[38] J. Gagné, L. Stamatatos, T. Diacovo, S.W. Hui, P.L. Yeagle, J.R. Silvius, Physical properties and surface interactions of bilayer membranes containing *N*-methylated phosphatidylethanolamines, Biochemistry 24 (1985) 4400–4408.
[39] A. Aroti, E. Leontidis, E. Maltseva, G. Brezesinski, Effects of Hofmeister anions on DPPC Langmuir monolayers at the air–water interface, J. Phys. Chem. B. 108 (2004) 15238–15245.
[40] M. Levitt, Symmetrical composite pulse sequences for NMR population inversion: I. Compensation of radiofrequency field inhomogeneity, J. Magn. Reson. 48 (1982) 234–264.
[41] S.M. Reutzel-Edens, J.K. Bush, P.A. Magee, G.A. Stephenson, S.R. Byrn, Anhydrates and hydrates of olanzapine: crystallization, solid-state characterization, and structural relationships, Cryst. Growth Des. 3 (2003) 897–907.
[42] C.F. Schmidt, Y. Barenholz, C. Huang, T.E. Thompson, Phosphatidylcholine $C_{13}$-labelled carbonyls as a probe of bilayer structure, Biochemistry 16 (1977) 3948–3954.
[43] B.A. Cornell, M. Keniry, The effect of cholesterol and gramicidin A′ on the carbonyl groups of dimyristoylphosphatidylcholine dispersions, Biochim. Biophys. Acta 732 (1983) 705–710.
[44] P.G. Scherer, J. Seelig, Electric charge effects on phospholipid headgroups. Phosphatidylcholine in mixtures with cationic and anionic amphiphiles, Biochem. 28 (1989) 7720–7728.
[45] J.S. Santos, D.-K. Lee, A. Ramamoorthy, Effects of antidepressant on the conformation of phospholipid headgroups studied by solid-state NMR, Mag. Res, Chem. 42 (2004) 105–114.
[46] M.R.R. de Planque, B.B. Bonev, J.A.A. Demmers, D.V. Greathouse, R.E. Koeppe II, F. Separovic, A. Watts, J.A. Killian, Interfacial anchor properties of tryptophan residues in transmembrane peptides can dominate over hydrophobic matching effects in peptide–lipid interactions, Biochem. 42 (2003) 5341–5348.
[47] S.P. Bhamidipatit, J.A. Hamilton, Interactions of Lyso 1-palmitoylphosphatidylcholine with phospholipids: a $^{13}$C and $^{31}$P NMR study, Biochemistry 34 (1995) 5666–5677.

[48] Olanzapine, Material Safety Data Sheet, Eli Lilly and Company, January 7th, 2008.
[49] A. Ramamoorthy, S. Thennarasu, A. Tan, D.-K. Lee, C. Clayberger, A.M. Krensky, Cell selectively correlates with membrane-specific interactions: a case study on the antimicrobial peptide G15 derived from granulysin, Bioch. Biophys. Acta 1758 (2006) 154–163.
[50] I. Wawrzycka-Gorczyca, P. Borowski, J. Osypiuk-Tomasik, L. Mazur, A.E. Koziol, Crystal structure of olanzapine and its solvates. Part 3. Two and three-component solvates with water, ethanol, butan-2-ol and dichloromethane, J. Mol. Struct. 830 (2007) 188–197.
[51] A. Jutila, T. Söderlund, A.L. Pakkanen, M. Huttunen, P.K.J. Kinnunen, Comparison of the effects of clozapine, chlorpromazine, and haloperidol on membrane lateral heterogeneity, Chem. Phys. Lipids 112 (2001) 151–163.
[52] S. Steinkopf, A.K. Schelderup, H.L. Gjerde, J. Pfeiffer, S. Thoresen, A.U. Gjerde, H. Holmsen, The psychotropic drug olanzapine (Zyprexa®) increases the area of acid glycerophospholipid monolayers, Biophys. Chem. 134 (2008) 39–46 (this issue), doi:10.1016/j.bpc.2008.01.003.